Geology, Geophysics & Environment 2025, vol. 51 (4): 323–335

Vertical variations in the concentration of traffic-related pollutants PM in a selected area along a transport corridor

Agata Jaroń[1], Anna Borucka[2]

[1] *Military University of Technology, Doctoral School, Warsaw, Poland, e-mail: agata.jaron@wat.edu.pl (corresponding author), ORCID ID: 0000-0001-5054-061X*
[2] *Military University of Technology, Faculty of Security, Logistics and Management, Warsaw, Poland, e-mail: anna.borucka@wat.edu.pl, ORCID ID: 0000-0002-7892-9640*

Received: 25 May 2025; accepted: 3 October 2025; first published online: 22 December 2025

Abstract: Profiling pollutant distributions contributes to a deeper understanding of the diffusion of traffic air pollution, with road transport being a significant source of air pollution. The available literature presents numerous methods for analyzing air pollution distributions resulting from vehicular transport. However, these studies primarily focus on simulated conditions rather than real-world field measurements. This study examines real-world field measurements of air pollution near a highway in Poland using an unmanned aerial vehicle (UAV) platform across different seasons. The UAV platform was equipped with a semiconductor laser sensor for measuring air pollutants such as SO_2, CO_2, N_xO_y, O_3 and PM_{10}, $PM_{2.5}$ and PM_1. Although there are many works on profiling pollutants, this is the first such attempt to visualize pollutants in Poland, along with comparing the indications to the National Air Pollution Monitoring. By applying Spearman's correlation coefficient, the study assesses the correlation of pollutant concentrations within the vertical profile from a street canyon and conducts pollution mapping. Observations indicate that in spring, summer, and autumn, pollutant concentrations decrease with altitude. However, in winter, a "pollution cloud" was detected at an altitude of 20–30 m, while concentrations above this threshold declined. The findings provide valuable insights for developing recommendations to protect public health. In the future, they may be used to properly manage urban infrastructure in order to protect the population from the negative effects of air pollution.

Keywords: traffic air pollution, UAV measurement, pollution profiling

INTRODUCTION

Road transport has become the third-largest contributor to global air pollution (Jiang et al. 2024). This has a significant impact on global climate issues and air quality, posing a threat to the sustainable development of humanity (Jiang et al. 2024). With economic growth, the number of vehicles and the demand for transport services continue to rise. Despite the significant expansion of the electric vehicle sector within the European Union, internal combustion engine vehicles still dominate the automotive market, both in Europe and globally (Vrublevskyi & Wierzbicki 2023). Observing the prevailing trends in Europe, it is difficult to predict a global shift in preferences toward transport solutions based on electric vehicles (Karpenko et al. 2025, Shivkumar et al. 2025). According to the European Environment Agency, one-fourth of total air pollution emissions originate from the transport sector, with nearly 72% coming from road transport (EEA n.d., Zheng et al. 2021).

The movement of vehicles generates the emission of harmful pollutants such as SO_x, NO_x, CO_2, VOCs, formaldehydes, and many others, as well as particulate matter such as PM_{10}, $PM_{2.5}$, PM_1, and ultrafine PM (Lee et al. 2021, Andrych-Zalewska et al. 2023, Kozak et al. 2025). It is important to emphasize that particulate matter pollution poses a significant threat to human health (Ivanova 2020). The ability of PM to penetrate the alveoli and enter the bloodstream contributes to numerous cardiovascular, respiratory diseases, and allergies (Olesiejuk & Chałubiński 2023). In Poland, air quality in large urban agglomerations is still unsatisfactory. Due to their high dispersion potential, air pollutants can spread over vast areas, causing negative effects on ecosystems. Increased exposure to high concentrations of harmful particles near transport corridors has a detrimental impact on human health. Therefore, understanding vertical pollution distribution patterns from road traffic emissions is crucial for ensuring sustainable human development. The obtained profiles can contribute to assessing environmental impact and serve as the basis for formulating recommendations to mitigate this adverse phenomenon. Analyzing such data facilitates the identification of the impact of transport systems on ecosystem health. These studies also support the development of effective strategies to minimize environmental damage. Implementing appropriate measures can help improve residents' quality of life and protect biodiversity, while regular monitoring and updates of pollution profiles will enable a faster response to emerging challenges.

LITERATURE REVIEW AND DEMONSTRATION OF THE VALIDITY OF THE TOPIC

The diffusion of pollutants caused by vehicle movement takes place in two dimensions: horizontal and vertical. The available literature has shown considerable interest in the horizontal movement of air pollutants. In study by Jaroń and Borucka (2024) the authors focused on examining the relationship between PM concentrations in different seasons of the year and the interval from the highway (distance), based on real-world field measurements using a UAV platform. The authors observed that correlation signs differed between summer and winter periods. Yang et al. (2022) applied numerical modeling to analyze the horizontal diffusion of traffic-related pollutants in relation to vertical wind gusts. The results demonstrated that horizontal movement and vertical wind gusts significantly contribute to the transport of pollutants over large areas. Draxler and Taylor (1982) discussed horizontal dispersion parameters, focusing on the definition and evaluation of dispersion model transport in order to assess the impact on health and the environment. Furthermore, the Gaussian model presented in the study assumed that pollutants disperse according to a normal distribution from the emission source. Li et al. (2006) applied computational fluid dynamics (CFD) to investigate pollutant dispersion within street canyons under various atmospheric conditions, wind directions, and terrain formations. This scientific approach allowed us to understand how air pollution caused by road transport changes over time and in different locations, where it is influenced by weather and terrain conditions. Vertical dispersion is extremely important as it contributes to the transport of pollutants over larger areas (Chaari et al. 2024). Researchers (Weber et al. 2006) studied vertical profiles within street canyons and demonstrated that air pollution decreases exponentially with altitude. Additionally, the authors provided evidence of similar behavior in suspended particles which are emitted as a result of combustion, tire wear, and brake abrasion. Conversely, Park et al. (2024) observed uniform pollutant particle profiles within street canyons. From the available sources it appears that there is a very limited number of works devoted to vertical dispersion in comparison to horizontal dispersion (Zhang et al. 2023, Frederickson et al. 2024). Understanding how air pollutants are distributed within the vertical column of the first few meters of the boundary layer across various urban environments is crucial for improving exposure assessment methods and enhancing strategies to protect human health. Current knowledge is based on general assumptions regarding pollutant concentration distribution across different environments. As a result, there is a research gap in observing variations in vertical pollution profiles under different atmospheric conditions (across different seasons) and

there is no indication of how these results correspond to the results provided by government institutions monitoring air pollution. Based on this, the following research question was formulated: Do traffic-related pollutant concentrations vary with height above the road surface over annual observations and how do the obtained results correspond to the results of government institutions monitoring air pollution? This investigation allowed for the determination of the impact of atmospheric conditions on pollutant dispersion in the vertical air profile. Additionally, it enabled the identification of key factors contributing to pollutant accumulation within a specific altitude layer.

MATERIALS AND METHODS

In order to answer the research question, a Yuneec Typhoon H Plus UAV platform was used. The total weight of the UAV is 1,645 g. The maximum speed of the UAV is 13.5 m/s. The UAV platform had a Mapair sensor, a laser-based PM_1, $PM_{2.5}$, and PM_{10} particle concentration sensor, along with semiconductor sensors for other pollutants from Winsen, Gravity, and SGX Sensortech. The values of all pollutants detected by the Mapair sensor are modified by a normalizing parameter, which represents pollutants for a reference atmosphere (288.15 K and 1,013.25 hPa), allowing for a direct comparison of pollutant levels across sensors regardless of atmospheric conditions. This is accomplished by collecting data from the weather station closest to the sensor. This data is used to calculate the normalizing parameter. This parameter is refreshed every 5 minutes to ensure accuracy and maximize the sensor's responsiveness. Additionally, the sensor is integrated with a GPS system, allowing for precise localization of measurement points, including longitude, latitude, and altitude above sea level. The GPS system is equipped with a UBLOX M10 chip, accuracy is 1.5 m CEP. Taking into account the technical specifications and the area under investigation, it can be stated that the obtained measurement data are characterized by a high degree of accuracy. The collected measurement points can also be visualized on a map, creating pollution maps. The UAV system used in the study is presented in Figure 1.

The study area covers 1 ha and is located on the A4 motorway in Katowice, Śląskie Voivodship, Poland and passes through a conurbation which is home to 280,000 people. The measurement location is shown in Figure 2 and contains two characteristic points, namely the UAV take-off and landing site and the reference point of the national pollution monitoring station. It's important to note that a national air pollution monitoring station is located in the study area.

Fig. 1. *UAV platform for measuring traffic-related pollution*

Fig. 2. *Study area marked with a yellow line*

Katowice has two such stations: one in the immediate vicinity and the other in the city center. Based on data from the national air pollution monitoring system, it can be seen that the highway significantly contributes to the increase in harmful pollutants, allowing for the elimination of other sources of pollution.

The determination of profiles is a continuation of previous research related to pollution mapping (Jaroń et al. 2024) and horizontal correlation analysis (Jaroń & Borucka 2024). The measurement data consist of air pollutant concentration values obtained from UAV surveys conducted over a full year under different atmospheric conditions (seasons). The measurement data obtained from the UAV platform include total pollutant concentrations, as the aim of the work was to capture the overall impact of traffic factors in the urban environment. The unmanned aerial vehicle performed measurements once for each season separately, i.e. once a quarter at the same time of day during the busiest time. The UAV flight lasted one hour. Taking into account the flight speed and measurement accuracy, the UAV performed measurements with an accuracy of 1 m, obtaining over 4,000 measurement values. The seasons are: winter, autumn, summer and spring. Spring was defined as the period when measurements were taken in May 2024 and the average temperature was 18°C air humidity was 29%. Summer measurements were taken in July, where the average temperature was 30°C and air humidity was 24%. Autumn measurements were taken in November, and the average temperature was 13°C and air humidity was 38%. Winter measurements were taken in January when the temperature was 0°C and the air humidity was 53%. The wind factor was excluded in the study by selecting measurement days where the weather phenomenon was "calm" i.e. a windless day, occurred for each of the measurement days. A preliminary assessment of the collected data was performed by Jaroń et al. (2024), where 3D maps enabled the observation of pollution variations with altitude. The preliminary observation inby Frederickson et al. 2024) showed that the concentration of pollutants other than PM_x is constant on the tested road section.

CORRELATION BETWEEN AIR POLLUTION VARIATIONS AND ALTITUDE

The UAV drone conducted measurements at various altitudes, specifically 10, 20, 30, 40, and 50 m above the terrain. The sensor mounted on the UAV is capable of quantitatively and qualitatively measuring eight types of air pollutants. However, after an initial review of pollution maps from

study by Jaroń and Borucka (2024), it was observed that significant variations in pollutant dispersion occurred only for suspended particulate matter (PM_{10}, $PM_{2.5}$, and PM_1). For pollutants such as HCHO, O_3, and SO_2, the concentration value at each measurement point was the same, while for PM pollutants, it was different. For better data visualization, Figures 3 and 4 present illustrative examples of pollution maps.

Figures 3 and 4 are for preliminary evaluation. Figure 3 shows the level of HCHO pollution, which is constant at each measurement point, while the PM concentration is different at each measurement point in Figure 4. Taking into account the above, further analysis focused on examining the relationship between the concentration of suspended particulate matter. In accordance with the study assumptions, a correlation analysis was performed to check whether PM concentrations change with altitude. Initially, it was verified whether distributions within the groups conformed to normal distributions.

Fig. 3. *Pollution map for HCHO*

Fig. 4. *Pollution map for $PM_{2.5}$*

The Lilliefors definition test was used, a statistical test used to check whether the analyzed data comes from a distribution close to normal. It allows the further direction of the analysis to be identified in order to determine the correlation. Table 1 shows the results of the test.

Table 1
Results of the Lilliefors test

Pollutant	Lilliefors test	*p*-value
PM_1	0.3581	$<2.2 \cdot 10^{-16}$
$PM_{2.5}$	0.3593	$<2.2 \cdot 10^{-16}$
PM_{10}	0.3575	$<2.2 \cdot 10^{-16}$

Analyzing Table 1, it can be concluded that all *p*-values are lower than the assumed significance level. Therefore, the measurement data do not have a normal distribution and thus the Spearman's correlation should be used.

The Spearman's correlation is a measure of the statistical relationship between random variables. In contrast to the Pearson's coefficient, which determines a linear relationship between variables and treats any other relationship as a disturbance of the linear relationship, rank correlation identifies any monotonic relationship, including nonlinear ones. Its application does not require assumptions of normality, and it is robust against outliers. If a sample contains unique elements, the simple rank is the position of the observation in the ordered sample. In cases with repeated elements, the same rank is assigned to each repeated element. Spearman's rank correlation coefficient is calculated using the following formula (Spearman 1904):

$$r_s = 1 - \frac{6\sum_{i=1}^{n} d_i^2}{n\left(n^2 - 1\right)} \tag{1}$$

where the difference between ranks is given by:

$$d_i = R_{x_i} - R_{y_i} \tag{2}$$

For n observations corresponding to realizations x_i, y_i of features X and Y. The coefficient takes a value from the interval <–1, 1>. Interpretation requires checking the significance using a statistical test.

Table 2
The determined correlation coefficient of individual PM concentrations with altitude for annual observations and the value of descriptive statistics

Pollutant	Correlation coefficient (*df* = 10,197)	Test statistic value	*p*-value
PM_1	–0.047	$1.851 \cdot 10^{11}$	$1.919 \cdot 10^{-6}$
$PM_{2.5}$	–0.048	$1.853 \cdot 11$	$1.181 \cdot 10^{-6}$
PM_{10}	–0.066	$1.885 \cdot 10^{11}$	$1.791 \cdot 10^{-11}$

Table 3
The determined correlation coefficient of individual PM concentrations with altitude for individual seasons and the value of descriptive statistics

Season	Correlation coefficient	Test statistic value	*p*-value
PM_1			
Spring	$r(1,547) = -0.227$	$7.616 \cdot 10^{8}$	$<2.2 \cdot 10^{-16}$
Summer	$r(3,618) = 0.168$	$6.571 \cdot 10^{9}$	$<2.2 \cdot 10^{-16}$
Autumn	$r(2,421) = -0.551$	$3.676 \cdot 10^{9}$	$<2.2 \cdot 10^{-16}$
Winter	$r(2,605) = -0.189$	$3.512 \cdot 10^{9}$	$<2.2 \cdot 10^{-16}$
$PM_{2.5}$			
Spring	$r(1,547) = -0.121$	$6.943 \cdot 10^{8}$	$1.794 \cdot 10^{-6}$
Summer	$r(3,618) = 0.111$	$7.031 \cdot 10^{9}$	$2.356 \cdot 10^{-6}$
Autumn	$r(2,421) = -0.521$	$3.607 \cdot 10^{9}$	$<2.2 \cdot 10^{-16}$
Winter	$r(2,605) = -0.222$	$3.609 \cdot 10^{9}$	$<2.2 \cdot 10^{-16}$
PM_{10}			
Spring	$r(1,547) = -0.114$	$6.901 \cdot 10^{8}$	$6.701 \cdot 10^{-6}$
Summer	$r(3,618) = 0.023$	$7.724 \cdot 10^{9}$	0.1669
Autumn	$r(2,421) = -0.577$	$3.739 \cdot 10^{9}$	$<2.2 \cdot 10^{-16}$
Winter	$r(2,605) = -0.244$	$3.674 \cdot 10^{9}$	$<2.2 \cdot 10^{-16}$

If *p*-value < α (where α = 0.05), the working hypothesis should be rejected and an alternative one accepted. Analyzing Tables 2 and 3, it can be concluded that for most samples, except for one (PM_{10} summer), correlations occur. If the correlation sign is negative, it means that the concentration decreases with height and vice versa. Table 2 shows that for all measurement data, particulate matter concentrations decrease with height above the road. However, Table 3 further reveals that concentrations decline across all analyzed seasons except for winter, where the correlation is positive. A graphical representation of the distributions as a function of height above sea level (m a.s.l.) for the entire year is shown in Figures 5–7, while Figures 8–10 illustrate the seasonal variations.

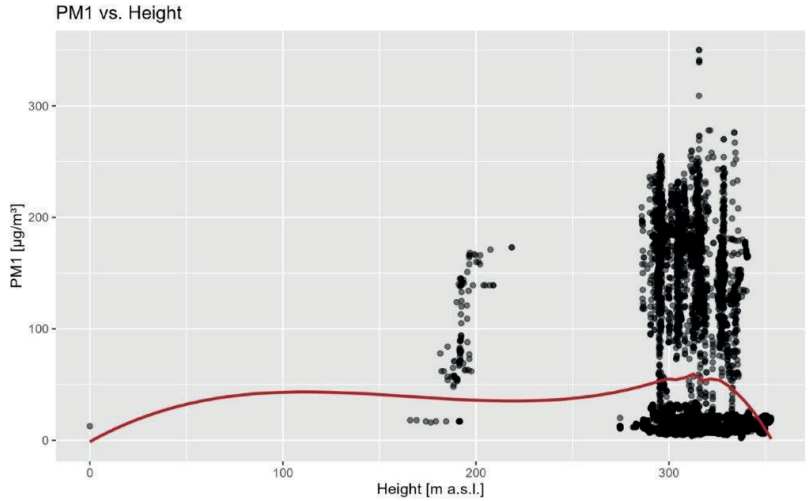

Figure 5. *Distribution of PM_1 concentration with altitude*

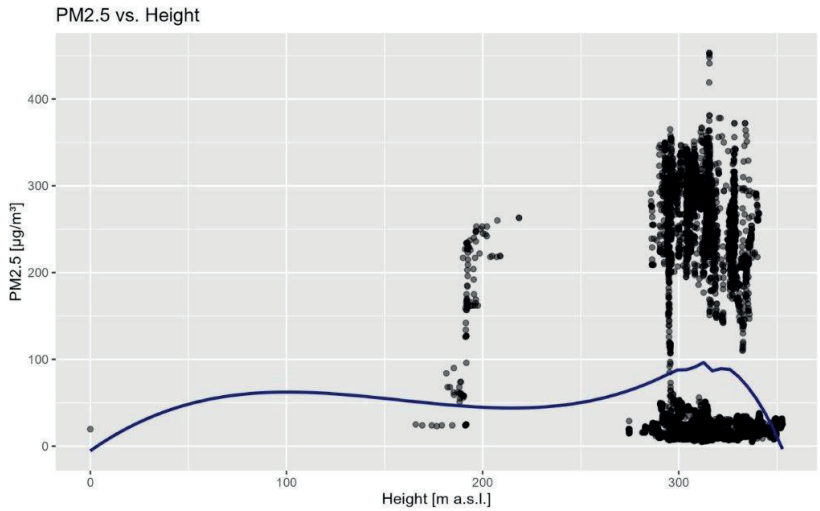

Fig. 6. *Distribution of $PM_{2.5}$ concentration with altitude*

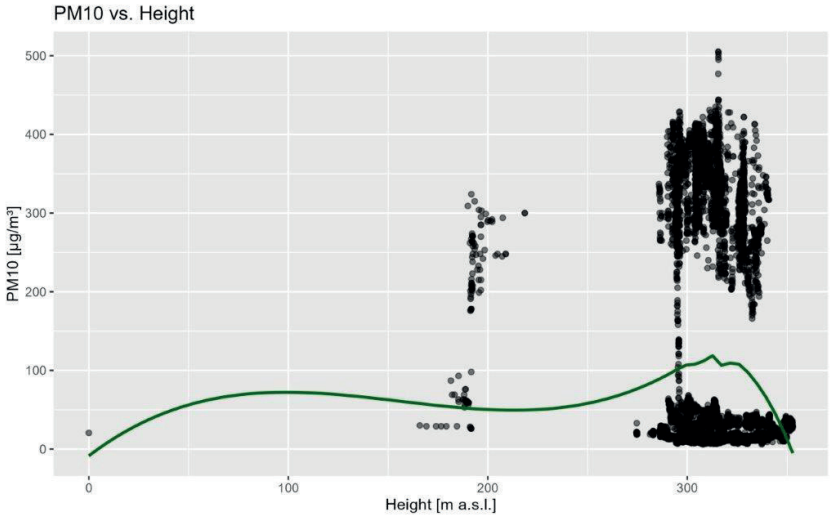

Fig. 7. *Distribution of PM_{10} concentration with altitude*

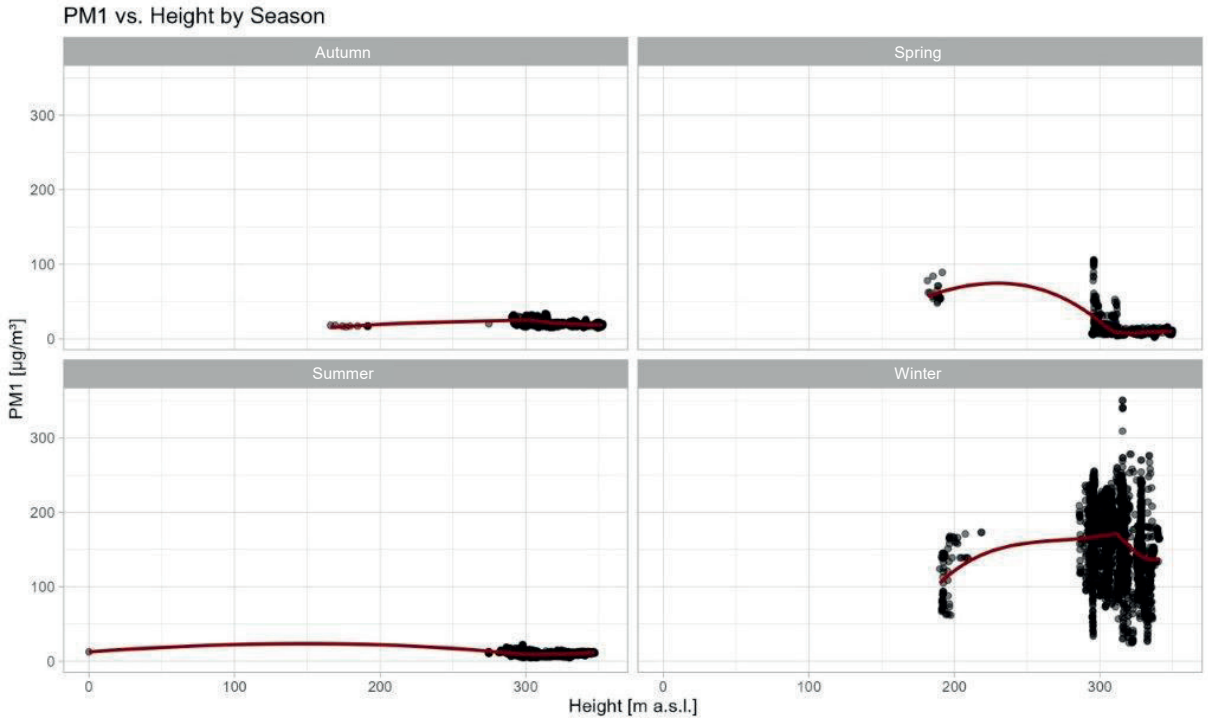

Figure 8. *Distribution of PM_1 concentration with altitude considering seasonality*

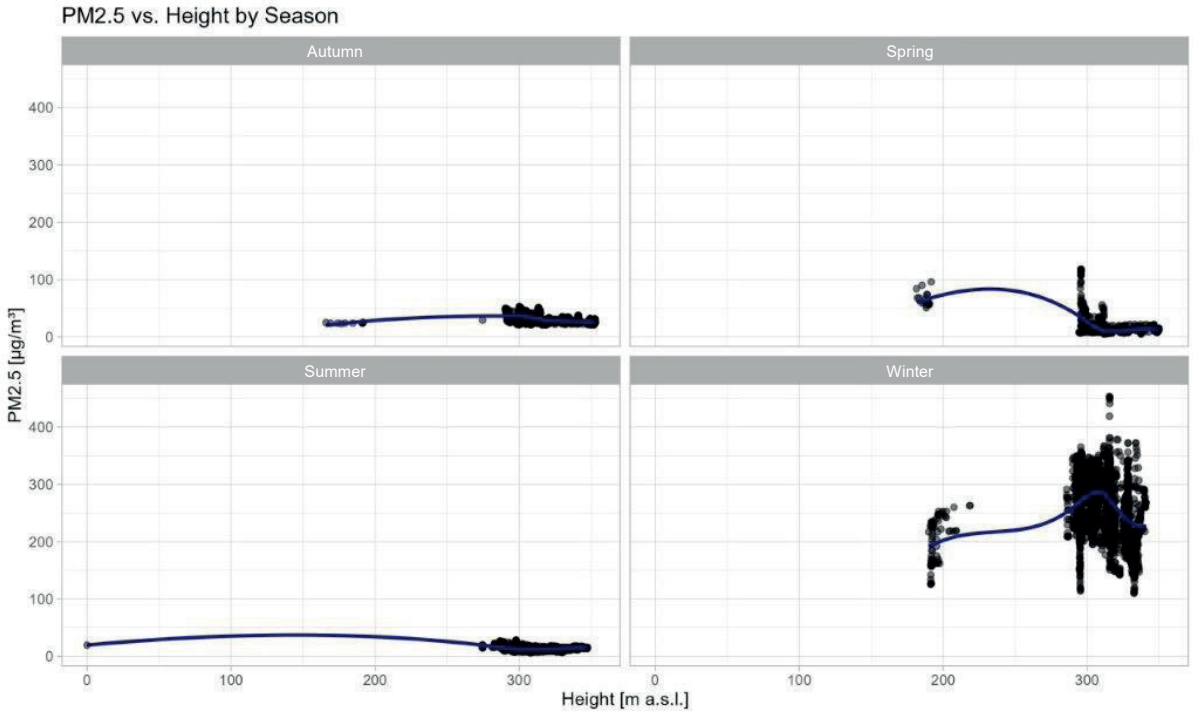

Fig. 9. *Distribution of $PM_{2.5}$ concentration with altitude considering seasonality*

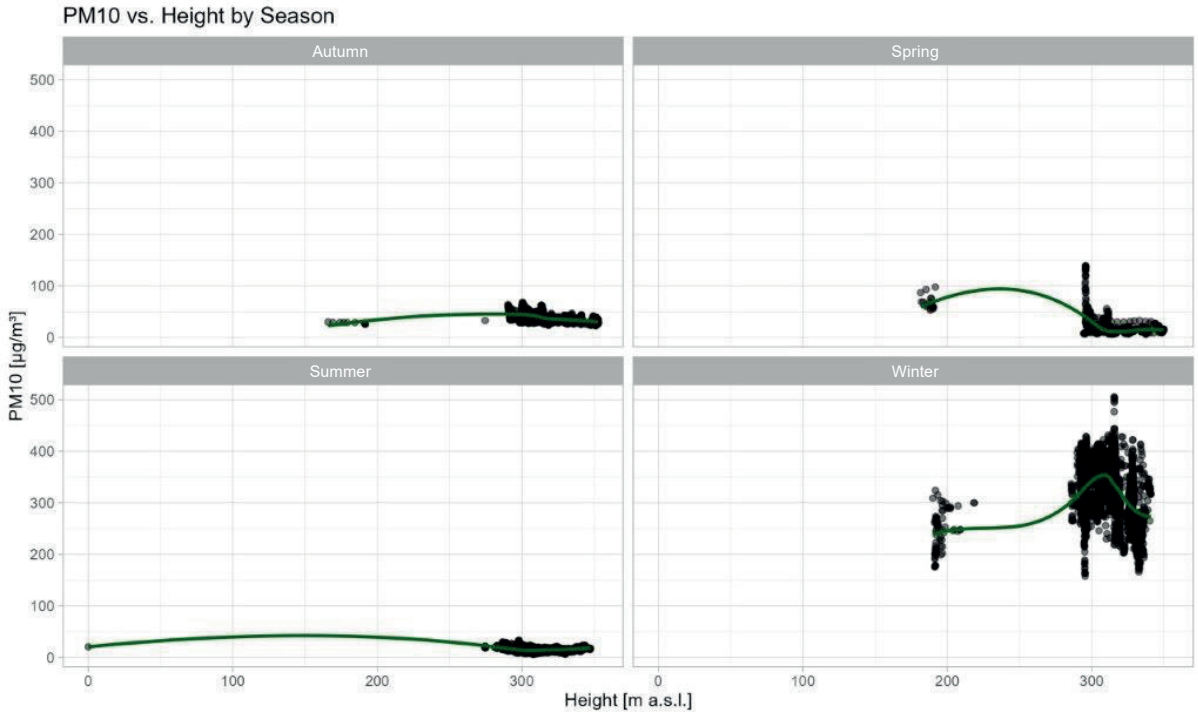

Fig. 10. *Distribution of PM_{10} concentration with altitude considering seasonality*

Analyzing Table 3 and Figures 5–10, a weak positive correlation is observed for the summer period (the red line is the regression line. The extension of the regression line to 0 m is intended only to illustrate the direction and nature of the observed trend and the presented trend line should not be interpreted as a forecast, but as a tool to aid in the interpretation of the observed trend.), indicating that pollutant concentration increases with altitude above the road. For the remaining periods, the correlation is negative, meaning that concentration decreases with increasing altitude. A similar phenomenon was described by Samad et al. (2020), who confirmed that air masses close to the ground were more polluted than air masses above. However, in their study, the authors took into account diurnal variations. It should be noted that the correlation coefficient values are low, specifically 0.023 for PM_{10}, 0.111 for $PM_{2.5}$ and 0.168 for PM_1. This can be explained by air humidity – it is the lowest in summer. Particulate matter absorbs water, increasing in mass, which facilitates its transport to lower altitudes. A similar process occurs in the formation of smog, where pollution clouds are easily transported to lower altitudes. The resulting phenomenon was also observed in the authors' studies described by Jaroń and Borucka (2024), in which horizontal correlations were studied. Additionally, similar observations are presented by Zheng et al. (2021), in which this phenomenon is called particle homogenization. However, after conducting a more detailed visualization of the vertical profile and mapping measurement points onto the terrain model using ArcGIS, it was noted that concentration increased up to a height of 15 m, after which it began to decline. An example of this profile is presented in Figure 11, which shows a projection of the pollution plane in height and width along the road.

The trend after 30 m is the result of changes in air humidity. At a height of about 30 m, the highest air humidity was observed. The humidity value at which the tendency decreased is 25%. High humidity causes the formation of an additional resistance layer, through which PM particles have difficulty breaking through and moving to higher distances.

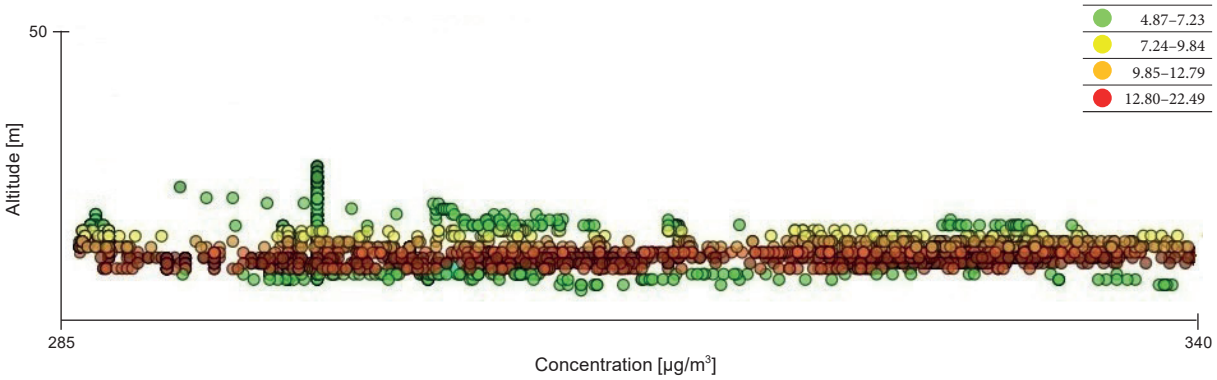

Fig. 11. *Vertical profile of PM in winter*

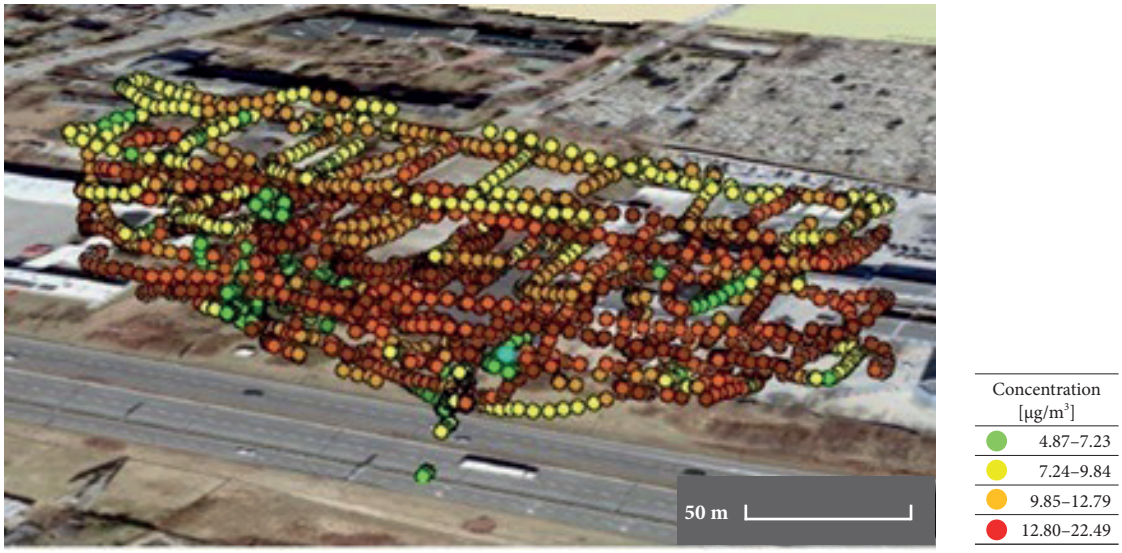

Fig. 12. *Vertical map of PM in summer*

Figure 11 corresponds to Figures 5–10 in that both show height profiles, however Figure 11 shows the projection along the distance scale along the X-axis and Figures 5–7 show the projections of the bracing along the height. Visualization helps to graphically present the occurring correlations. The correlation is weak and why it increases at first and then decreases.

Conversely, after mapping the summer period data, a increase in PM concentrations across the entire vertical profile can be observed (Fig. 12). The increase in PM concentration in the summer is associated with a period of increased temperatures and decreased humidity (humidity = 10%). The less humidity in the air, the easier it is to spread in the air and the greater the dispersal. In addition, the role of static stability must be taken into account. Unstable conditions favor vertical dispersion (e.g. spring or summer), stable conditions prevent vertical dispersion (e.g. winter, autumn). It should be emphasized that the measurements were not taken above the street but near the adjacent area.

DISCUSSION

The measurement site was not chosen randomly. Its selection was based on the proximity of a monitoring station operated by the Chief Inspectorate of Environmental Protection, allowing for a comparison between the obtained results and official government measurements. It should be noted that the UAV platform conducted measurements at five different altitudes: 10, 20, 30, 40, and 50 m above the terrain. The height of the national

environmental monitoring station is 5–8 m. The UAV measurements and the average values across these five altitudes are presented in Table 4. The GIOS column presented in this table contains the results obtained from the national air pollution monitoring measurements.

Table 4 shows that the highest emission is in winter. This is a normal phenomenon caused by seen that throughout the year, except for summer, the concentration decreases with altitude. In winter, there is a noticeable increase in concentration at a height of 30 m and then a decrease, which is consistent with the phenomenon described in Chapter "Analysis of correlation between air pollution variations and altitude."

With the UAV measurement values at various altitudes *H* and the results from GIOŚ, it is possible to calculate the relative measurement error using the following formula:

$$\Delta x = \left| x - x_0 \right| \tag{3}$$

where x represents the exact value, and x_0 represents the measured value. The absolute error is defined as:

$$\delta = \frac{\left| x - x_0 \right|}{x} \cdot 100\% \tag{4}$$

The measurement error results at different altitudes relative to GIOŚ measurements are presented in Table 5.

Table 4
Comparison of UAV measurements and altitude-based data

Season	GIOŚ results	10 m	20 m	30 m	40 m	50 m
PM_{10} [µg/m^3]						
Spring	17.48	17.23	16.98	15.01	13.21	12.85
Summer	15.94	15.60	14.30	13.45	11.11	10.51
Autumn	38.67	40.25	48.52	45.21	43.65	42.52
Winter	320.50	317.52	320.20	380.50	290.51	275.96
$PM_{2.5}$ [µg/m^3]						
Spring	15.45	15.20	14.92	13.52	12.58	11.85
Summer	13.24	12.30	11.92	10.83	10.85	10.52
Autumn	31.16	29.30	27.52	26.85	25.21	24.23
Winter	262.04	270.00	290.90	320.52	275.62	252.12
PM_1 [µg/m^3]						
Spring	–	14.52	14.25	13.85	13.21	12.85
Summer	–	12.62	11.89	11.62	10.87	10.26
Autumn	–	33.54	32.65	31.25	30.45	29.85
Winter	–	38.21	29.42	42.10	35.41	31.89

"–" not subject to measurement.

Table 5
Difference in relation to the reference measurement

Season	Δ_1	Δ_2	Δ_3	Δ_4	Δ_5
PM_{10} [%]					
Spring	1.45	2.94	14.79	18.54	26.81
Summer	2.17	3.59	15.98	19.71	27.97
Autumn	3.93	4.34	10.97	11.15	6.32
Winter	0.93	0.09	24.94	10.22	9.88
$PM_{2.5}$ [%]					
Spring	1.64	3.55	10.35	18.61	26.16
Summer	4.64	5.07	9.96	12.86	15.13
Autumn	6.34	8.22	12.49	13.16	15.04
Winter	2.94	18.34	20.45	8.42	5.32

Analyzing Table 5, it can be observed that at lower altitudes, specifically 10 and 20 m, which are close to the height of the monitoring station, the measurement error is only a few percent and remains relatively small. However, as altitude increases, the measurement error also increases, except during the winter period, where the error initially rises but then decreases after exceeding $H = 30$ m. At the altitude and latitude of the place where measurements are taken in the winter, the phenomenon of "smog" occurs, these are pollutants suspended in the air. Due to the fact that smog occurs, the pollutants are evenly distributed, which is why the measurement error does not increase with altitude (Guo et al. 2023, Jaroń & Borucka 2024).

CONCLUSION

Motor vehicle traffic is a significant source of air pollution. Moreover, due to its high diffusion capacity, traffic-related pollution has become a global issue. Considering this, it is crucial to illustrate the causes of this environmental problem and its implications.

In Poland, the available national measurement methods rely on averaged point measurements at a single altitude, which creates a significant discrepancy compared to surface-based measurements. As demonstrated in this study, this approach results in a substantial measurement error. Such measurements do not accurately reflect the actual risk and fail to properly describe the prevailing environmental conditions.

Analyzing the available literature on the dispersion of pollutants emitted from traffic sources, numerous studies focus on modelling and numerical methods to simulate the spread of pollutant particles. However, there are few studies dedicated to real-world field measurements, particularly those considering vertical profiling, which – according to the literature – has the greatest influence on the range of pollution dispersion. The aim of this study is to determine whether the concentrations of road traffic-related pollutants change with height above the road surface. Using the Spearman's correlation coefficient, it was observed that during spring, winter, and autumn, the correlation is negative, meaning that pollutant concentrations decrease with height distance from the road. The exception is summer, where the correlation is weak and positive. Additionally, an analysis of pollution profile mapping revealed that pollutant accumulation is highest between 20 and 30 m in altitude before gradually dissipating.

The air humidity has an influence on the described phenomenon, which is increased as described in Chapter "Analysis of correlation between air pollution variations and altitude." The reference point is also the publication by Jaroń and Borucka (2024) where horizontal profiles were studied in a similar way. A similar relationship was observed during the annual observation period, which confirms the clear influence of air humidity on PM diffusion.

Attention should also be given to the comparison of GIOŚ results with UAV platform measurements, where it can be observed that at the measurement altitude corresponding to the station's height, the measurement error is minimal (a few percent). However, as the distance increases, the error grows, which is directly related to changes in pollutant distribution patterns.

In summary, the measurement method described in this study serves as a valuable source of information on vertical profiling of traffic-related pollution. The findings obtained will contribute to developing recommendations for protecting the population from the harmful effects of pollutant dispersion, similar to the approach taken in constructing protective noise and vibration barriers along highways.

We would like to thank DronePol for providing the UAV platform used to perform the measurements.

REFERENCES

Adamiak B., Andrych-Zalewska M., Merkisz J. & Chłopek Z., 2025. The uniqueness of pollutant emission and fuel consumption test results for road vehicles tested on a chassis dynamometer. *Eksploatacja i Niezawodność – Maintenance and Reliability*, 27(1), 195747. https://doi.org/10.17531/ein/195747.

Andrych-Zalewska M., Chlopek Z., Pielecha J. & Merkisz J., 2023. Investigation of exhaust emissions from the gasoline engine of a light duty vehicle in the Real Driving Emissions test. *Eksploatacja i Niezawodność – Maintenance and Reliability*, 25(2), 165880. https://doi.org/10.17531/ein/165880.

Andrych-Zalewska M., Chłopek Z., Merkisz J. & Pielecha J., 2024. Research on the results of the WLTP procedure for a passenger vehicle. *Eksploatacja i Niezawodność – Maintenance and Reliability*, 26(1), 176112. https://doi.org/10.17531/ein/176112.

Chaari A., Mouhali W., Sellila N., Louaked M. & Mechkour H., 2024. Pollutant dispersion dynamics under horizontal wind shear conditions: Insights from bidimensional traffic flow models. *Fluids*, 9(11), 265. https://doi.org/10.3390/fluids9110265.

Draxler R.R. & Taylor A.D., 1982. Horizontal dispersion parameters for long-range transport modeling. *Journal of Applied Meteorology and Climatology*, 21(3), 367–372. https://doi.org/10.1175/1520-0450(1982)021<0367:HDPFLR>2.0.CO;2.

European Environment Agency (EEA), n.d. *Indicators*. https://www.eea.europa.eu/data-and-maps/indicators/transport-emissions-of-air-pollutants-8/transport--emissions-of-air-pollutants-4 [access: 2.02.2024].

Frederickson L.B., Russell H.S., Raasch S., Zhang Z., Schmidt J.A., Johnson M.S. & Hertel O., 2024. Urban vertical air pollution gradient and dynamics investigated with low-cost sensors and large-eddy simulations. *Atmospheric Environment*, 316, 120162. https://doi.org/10.1016/j.atmosenv.2023.120162.

Guo L., Han X., Li Y., 2023. The smog that hovers: Air pollution and asset prices. *Finance Research Letters*, 53, 103633. https://doi.org/10.1016/j.frl.2023.103633.

Ivanova V.R., 2020. The anthropogenic air pollution and human health. *Journal of IMAB – Annual Proceeding (Scientific Papers)*, 26(2), 3057–3062. https://doi.org/10.5272/jimab.2020262.3057.

Jaroń A. & Borucka A., 2024. Spatiotemporal changes in air pollution within the studied road segment. *Sustainability*, 16(17), 7292. https://doi.org/10.3390/su16177292.

Jaroń A., Borucka A., Deliś P. & Sekrecka A., 2024. An assessment of the possibility of using unmanned aerial vehicles to identify and map air pollution from infrastructure emissions. *Energies*, 17(3), 577. https://doi.org/10.3390/en17030577.

Jiang Z., Wu L., Niu H., Jia Z., Qi Z., Liu Y., Zhang Q., Wang T., Peng J. & Mao H., 2024. Investigating the impact of high-altitude on vehicle carbon emissions: A comprehensive on-road driving study. *Science of The Total Environment*, 918, 170671. https://doi.org/10.1016/j.scitotenv.2024.170671.

Karpenko M., Prentkovskis O. & Skačkauskas P., 2025. Analysing the impact of electric kick-scooters on drivers: vibration and frequency transmission during the ride on different types of urban pavements. *Eksploatacja i Niezawodność – Maintenance and Reliability*, 27(2), 199893. https://doi.org/10.17531/ein/199893.

Kozak M., Waligórski M., Wcisło G., Wierzbicki S. & Duda K., 2025. Exhaust emissions from a direct injection spark-ignition engine fueled with high-ethanol gasoline. *Energies*, 18(3), 454. https://doi.org/10.3390/en18030454.

Lee Y.-G., Lee P.-H., Choi S.-M., An M.-H. & Jang A.-S., 2021. Effects of air pollutants on airway diseases. *International Journal of Environmental Research and Public Health*, 18(18), 9905. https://doi.org/10.3390/ijerph18189905.

Li X.-X., Liu C.-H., Leung D.Y. & Lam K.M., 2006. Recent progress in CFD modelling of wind field and pollutant transport in street canyons. *Atmospheric Environment*, 40(29), 5640–5658. https://doi.org/10.1016/j.atmosenv.2006.04.055.

Olesiejuk K. & Chałubiński M., 2023. How does particulate air pollution affect barrier functions and inflammatory activity of lung vascular endothelium? *Allergy*, 78(3), 629–638. https://doi.org/10.1111/all.15630.

Park S.-K., Kim S.-D. & Lee H., 2004. Dispersion characteristics of vehicle emission in an urban street canyon. *Science of The Total Environment*, 323(1–3), 263–271. https://doi.org/10.1016/j.scitotenv.2003.09.032.

Samad A., Vogt U., Panta A. & Uprety D., 2020. Vertical distribution of particulate matter, black carbon and ultra-fine particles in Stuttgart. *Atmospheric Pollution Research*, 11(8), 1309–1042. https://doi.org/10.1016/j.apr.2020.05.017.

Shivkumar P., Evangeline J.S., Bagyalakshmi B.K. & Murugan M.T., 2025. Improving reliability in electric vehicle battery management systems through deep learning-based cell balancing mechanisms. *Eksploatacja i Niezawodność – Maintenance and Reliability*, 27(3), 200714. https://doi.org/10.17531/ein/200714.

Spearman C., 1904. The proof and measurement of association between two things. *The American Journal of Psychology*, 15(1), 72–101. https://doi.org/10.2307/1412159.

Vrublevskyi O. & Wierzbicki S., 2023. Analysis of potential improvements in the performance of solenoid injectors in diesel engines. *Eksploatacja i Niezawodność – Maintenance and Reliability*, 25(3), 166493. https://doi.org/10.17531/ein/166493.

Weber S., Kuttler W. & Weber K., 2006. Flow characteristics and particle mass and number concentration variability within a busy urban street canyon. *Atmospheric Environment*, 40(39), 7565–7578. https://doi.org/10.1016/j.atmosenv.2006.07.002.

Yang H., Lu C., Hu Y., Chan P.-W. & Li L., 2022. Effects of horizontal transport and vertical mixing on nocturnal ozone pollution in the Pearl River Delta. *Atmosphere*, 13(8), 1318. https://doi.org/10.3390/atmos13081318.

Zhang S., Wang S., Xue R., Zhu J., He S., Duan Y., Huo J. & Zhou B., 2023. Impacts of Omicron associated restrictions on vertical distributions of air pollution at a suburb site in Shanghai. *Atmospheric Environment*, 294, 119461. https://doi.org/10.1016/j.atmosenv.2022.119461.

Zheng T., Li B., Li X.-B., Wang Z., Li S.-Y. & Peng Z.-R., 2021. Vertical and horizontal distributions of traffic-related pollutants beside an urban arterial road based on unmanned aerial vehicle observations. *Building and Environment*, 187, 107401. https://doi.org/10.1016/j.buildenv.2020.107401.